Research Article

Structure–activity relationships of resveratrol and derivatives in breast cancer cells

Rosamaria Lappano[1], Camillo Rosano[2], Antonio Madeo[1], Lidia Albanito[1], Pierluigi Plastina[3], Bartolo Gabriele[3], Luca Forti[4], Lucia Anna Stivala[5], Domenico Iacopetta[1], Vincenza Dolce[1], Sebastiano Andò[6], Vincenzo Pezzi[1] and Marcello Maggiolini[1]

[1] Dipartimento Farmaco-Biologico, Università della Calabria, Rende (CS), Italy
[2] Dipartimento di Bioinformatica e Proteomica Strutturale, Istituto Nazionale per la Ricerca sul Cancro (IST), Genova, Italy
[3] Dipartimento di Scienze Farmaceutiche, Università della Calabria, Rende (CS), Italy
[4] Dipartimento di Chimica, Università di Modena e Reggio Emilia, Modena, Italy
[5] Dipartimento di Medicina Sperimentale, Università di Pavia, Pavia, Italy
[6] Dipartimento di Biologia Cellulare, Università Della Calabria, Rende (CS), Italia

Resveratrol (RSV) is classified as a phytoestrogen due to its ability to interact with estrogen receptors (ERs). We assessed structure–activity relationships of RSV and the analogs 4,4′-dihydroxystilbene (4,4′-DHS), 3,5-dihydroxystilbene (3,5-DHS), 3,4′-dihydroxystilbene (3,4′-DHS), 4-hydroxystilbene (4-HS) using as model systems the ERα-positive and negative MCF7 and SkBr3 breast cancer cells, respectively. In binding assays and transfection experiments RSV and the analogs showed the following order of agonism for ERα: 3,4′-DHS > 4,4′-DHS > 4-HS > RSV, while 3,5-DHS did not elicit any ligand properties. Computational docking analysis and real-time PCR revealed for each analog a distinct ERα binding orientation and estrogen target gene expression profile. Interestingly, the aforementioned order of ligand activity was confirmed in proliferation assays which also showed the lack of growth stimulation by 3,5-DHS. Our data suggest that subtle changes in the structure of the RSV derivatives examined may be responsible for the different ERα-mediated biological responses observed in estrogen-sensitive cancer cells.

Keywords: Breast cancer / Docking analysis / Estrogen receptor / Hydroxystilbenes / Resveratrol

Received: July 25, 2008; revised: October 14, 2008; accepted: October 18, 2008

1 Introduction

Breast cancer is the most frequent tumor and the major cause of death among women in the United States [1]. The proliferation of many breast tumor cells is stimulated by the binding of 17β-estradiol (E2) to the estrogen receptor (ER) isoforms, ERα and ERβ, which belong to the nuclear receptor super-family. The transcriptional activity of the ERs is mediated by both an N-terminal ligand-independent activation function (AF-1) and a ligand-dependent activation function (AF-2) located in the ligand binding domain (LBD) [2]. The LBD contains a molecular switch helix–helix 12-which regulates the communication between ligand- and coactivator-binding sites [2, 3]. In ERα, as in other steroid hormone receptors, the ligand-binding pocket is a compact ellipsoid cavity, closely resembling the surface of the steroid ligands [4]. In the presence of agonist ligands, helix 12 is stabilized in a conformation that allows it to form one side of the coactivator-binding site and to completely encapsulate the ligand in the pocket. Antagonist ligands, such as the selective ER modulator (SERM) tamoxifen, resemble agonist ligands but contain an additional extended group [2–4]. The bulky side chain on tamoxifen protrudes between helices 3 and 11, and physically obstructs helix 12 from adopting the agonist conformation, thus preventing coactivator recruitment to the LBD [3]. The binding of E2 to the LBD of ERα induces conformational changes allowing receptor–chromatin interaction and the transcriptional regulation of target genes [5, 6]. A large body of data indicates that dietary factors play a sig-

Correspondence: Professor Marcello Maggiolini, Department Pharmaco-Biology, University of Calabria, 87030 Rende (CS), Italy
E-mail: marcellomaggiolini@yahoo.it
Fax: +390-984493458

Abbreviations: 4-HS, 4-hydroxystilbene; **CS,** charcoal-stripped; **DHS,** dihydroxystilbene; **E2,** 17β-estradiol; **ER,** estrogen receptor; **ICI,** ICI 182,780; **LBD,** ligand binding domain; **PR,** progesterone receptor; **RSV,** resveratrol

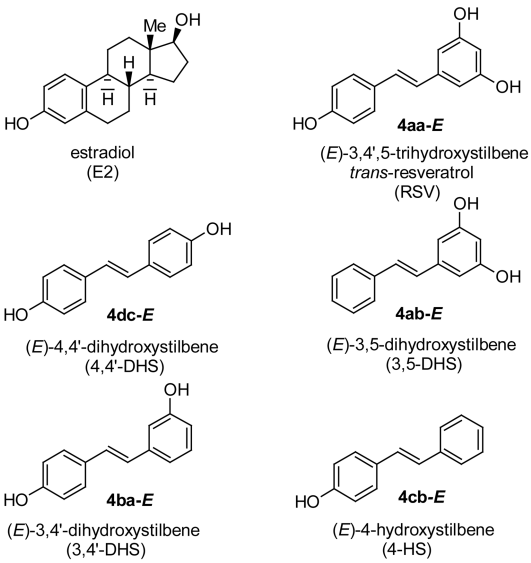

Figure 1. Chemical structures of E2, 3,4′,5-trihydroxystilbene (RSV), 4,4′-dihydroxystilbene (4,4′-DHS), 3,5-dihydroxystilbene (3,5-DHS), 3,4′-dihydroxystilbene (3,4′-DHS), and 4-HS.

nificant role in breast tumor development [7, 8]. For example, the low incidence of breast cancer in Asian women, who consume a high soy diet containing a significant amount of phytoestrogens [9], has been associated with the possibility that phytoestrogens may antagonize the effects of E2 [10]. However, there is no conclusive evidence that phytoestrogens act as antiestrogens [11–13]. Another possibility is that phytoestrogens exert antiproliferative and cancer-protective effects through an ER-independent pathway [14, 15].

Resveratrol (RSV) (Fig. 1) is a phytoalexin predominantly ingested with red grapes, peanuts, and berries [16–18]. RSV has been classified as a phytoestrogen due to its ability to interact with ERα and ERβ [6, 19–21]. On the basis of the estrogenic and antiestrogenic properties, RSV has also been considered a selective ER-modulator [19, 22–24]. It has been shown that high RSV levels may exert an antiproliferative effect in breast cancer cells regardless their ER status [25–27]. However, as reported for other phytoestrogens [6, 21, 28, 29], a biphasic response to RSV on cell growth has been reported depending on the concentration of RSV exposure. To date, the chemopreventive and cardioprotective effects of RSV have been attributed to its antioxidant and anticoagulant properties [30, 31].

Despite our detailed knowledge on the activities elicited by RSV through ERα, much less is known regarding whether different analogs of RSV could be accommodated in the receptor binding cavity and consequently induce the expression of genes such as pS2, Cathepsin D, progesterone receptor (PR), c-*fos*, Cyclin A, Cyclin D1, largely involved in the biological response to estrogens [32–34].

Using an *in vitro* screening model based on ERα-positive MCF7 and ER-negative SkBr3 breast cancer cells, we have investigated the structure–activity relationships of RSV and four hydroxystilbene analogs (Fig. 1), which were synthesized to assess the influence of the number and position of the hydroxyl groups present in the aromatic ring(s).

2 Materials and methods

2.1 Chemistry

Melting points were determined with a Reichert Thermovar apparatus and are uncorrected. ^{1}H NMR and ^{13}C NMR spectra were recorded at 25°C on a Bruker DPX Avance 300 or on a Bruker DPX Avance 500 spectrometer in $CDCl_3$ or DMSO-d_6 solutions at 300 or 500 and 75 or 126 MHz, respectively, with Me_4Si as internal standard. Chemical shifts (δ) and coupling constants (*J*) are given in ppm and in Hz, respectively. IR spectra were taken with a Perkin-Elmer Paragon 1000 PC FT-IR spectrometer. Mass spectra were obtained using a Shimadzu QP-2010 GC-MS apparatus at 70 eV ionization voltage. Microanalyses were carried out with a Carlo Erba Elemental Analyzer Mod. 1106. All reactions were analyzed by TLC on silica gel 60 F_{254} and by GLC using a Shimadzu GC-2010 gas chromatograph and capillary columns with polymethylsilicone + 5% phenylsilicone as the stationary phase (HP-5). Column chromatography was performed on silica gel 60 (Merck, 70–230 mesh). Evaporation refers to the removal of solvent under reduced pressure.

2.1.1 General procedure for the preparation of hydroxystilbenes 4aa-*E* (RSV), 4ab-*E*, 4ba-*E*, and 4cb-*E*

First step: Wittig reaction followed by isomerization to give methoxystilbenes 3-E. To a solution of 2 (4.4 mmol) and *t*-BuOK (494 mg, 4.4 mmol) in anhydrous THF (50 mL) maintained under nitrogen at –10°C with stirring was added 1 (dropwise in the case of 1b and 1c, in small portions in the case of 1a) (3.67 mmol). After additional stirring at –10°C under nitrogen for 1 h, the mixture was poured into water (*ca*. 100 mL). The resulting mixture was neutralized with 1 N HCl and then extracted with diethyl ether (3 × 20 mL). The collected organic phases were dried over Na_2SO_4. After filtration, the solvent was evaporated and the residue purified by column chromatography on silica gel, using 8:2 hexane–Et_2O (3aa, 3ba) or 9:1 hexane–Et_2O (3ab, 3cb) as eluent, to give 3 as an *E* + *Z* mixture. To a solution of 3 (*Z* + *E* mixture) in THF (50 mL) maintained under nitrogen with stirring was added PhSSPh (120 mg, 0.55 mmol in the case of 3aa; 143 mg, 0.65 mmol in the case of 3ab; 156 mg, 0.71 mmol in the case of 3ba; 68 mg, 0.31 mmol in the case of 3cb) and the resulting mixture was allowed to reflux for 1 h (in the case of 3aa), 2 h (in the case of 3ba), 4 h (in the case of 3ab), 6 h (in the case of 3cb). The solvent was evaporated and the residue was purified by column chromatography on silica gel using 8:2 hexane–Et_2O

(3aa, 3ba) or 9:1 hexane – Et_2O (3ab, 3cb) as eluent, to give pure isomers 3-*E*. The yields obtained in each case (based on starting 1) together with the characterization data for compounds 3-*E* are given below.

Second step: Deprotection of methoxystilbenes 3-E to give hydroxystilbenes 4-E. To a solution of 3-*E* (1.43 mmol) in anhydrous CH_2Cl_2 (30 mL) maintained under nitrogen at –20°C with stirring was added BBr_3 dropwise (2.51 g, 10.0 mmol in the case of 3aa-*E*, 3ab-*E*, and 3ba-*E*; 1.07 g, 4.27 mmol in the case of 3cb-*E*). The mixture, maintained under nitrogen with stirring, was allowed to warm up to room temperature (*ca*. 4 – 5 h), and then it was poured into water (*ca*. 100 mL) and extracted with AcOEt (3 × 20 mL). The collected organic phases were washed with brine (20 mL) and then dried over Na_2SO_4. After filtration, the solvent was evaporated and the residue purified by column chromatography on silica gel using 6:4 hexane – acetone (4aa-*E*), 7:3 hexane – AcOEt (4ab-*E*, 4ba-*E*), 8:2 hexane – AcOEt (4cb-*E*) as eluent, to give pure 4-*E*. The yields obtained in each case (based on 3-*E*) together with the characterization data for compounds 4-*E* are given below.

2.1.2 Preparation of (*E*)-4,4′-dihydroxystilbene 4cd-*E* (stilbestrol)

A mixture of 4-hydroxybenzaldehyde 1d′ (1.04 g, 8.52 mmol), 4-hydroxyphenylacetic acid 2c′ (1.96 g, 12.88 mmol), Ac_2O (15 mL), and Et_3N (3 mL) was heated at 180°C under nitrogen for 6 h. After cooling to room temperature, 5% HCl (30 mL) and AcOEt (30 mL) were added to the mixture. Phases were separated, and the aqueous layer was extracted with AcOEt (3 × 30 mL). The collected organic phases were washed with brine (50 mL) and dried over $MgSO_4$. After filtration, the solvent was removed under reduced pressure to obtain diacetylated α-(*p*-hydroxyphenyl)-*p*-hydroxycinnamic acid, which was then deacetylated at room temperature with K_2CO_3 in MeOH. After removal of the solvent under reduced pressure, the residue was diluted with 5% HCl (30 mL) and AcOEt (30 mL). Phases were separated, and the aqueous layer was extracted with AcOEt (3 × 30 mL). The collected organic phases were washed with brine (50 mL) and dried over $MgSO_4$. After filtration, the solvent was removed under reduced pressure to obtain crude α-(*p*-hydroxyphenyl)-*p*-hydroxycinnamic acid. Quinoline (12 mL) and $CuCrO_3$ (500 mg) were added to crude α-(*p*-hydroxyphenyl)-*p*-hydroxycinnamic acid (2.5 g), and the reaction flask was heated at 240°C under nitrogen for 5 h. After cooling, the mixture was filtered through celite and washed with AcOEt (2 × 30 mL). The filtrate was washed with 5% HCl (2′ × 30 mL) and dried over $MgSO_4$. After filtration, the solvent was removed under reduced pressure. The black oil thus obtained was purified by chromatography on silica gel using petroleum ether – AcOEt from 8:2 to 6:4 as the eluent, to give pure (*E*)-4,4′-dihydroxystilbene 4dc-*E* as an off-white solid (430 mg, 24% based on starting 1d′).

(E)-3,4′,5-Trimethoxystilbene (3aa-E). Yield: 735 mg, starting from 610 mg of 3,5-dimethoxybenzaldehyde (74%). Colorless solid, mp 56°C, lit. [35] 55 – 56°C. IR (KBr): ν = 3074 (w), 2991 (m), 2934 (m), 2834 (m), 1592 (s), 1511 (m), 1460 (m), 1279 (m), 1251 (m), 1071 (m), 1033 (m), 955 (m), 859 (m), 773 (m) cm^{-1}; ^1H NMR (500 MHz, $CDCl_3$): δ = 7.42 – 7.38 (m, 2 H, H-2′ + H-6′), 7.01 (distorted d, *J* = 16.5, 1 H, C*H*=CH), 6.87 (distorted d, *J* = 16.5, 1 H, CH=C*H*), 6.87 – 6.83 (m, 2 H, H-3′ + H-5′), 6.63 (d, *J* = 2.2, 2 H, H-2 + H-6), 6.36 (t, *J* = 2.2, 1 H, H-4), 3.77 (s, 6 H, 2 OCH_3), 3.75 (s, 3 H, OCH_3); ^{13}C NMR (126 MHz, $CDCl_3$): δ = 161.0, 159.4, 139.7, 129.9, 128.7, 127.8, 126.5, 114.1, 104.3, 99.6, 55.25, 55.20; GC-MS: *m/z* = 270 (100) [M^+], 269 (17), 255 (6), 239 (14), 227 (6), 224 (10), 212 (8), 197 (6), 196 (10), 195 (9), 181 (7), 169 (8), 165 (8), 153 (11), 152 (14), 141 (8), 115 (8); anal. calcd for $C_{17}H_{18}O_3$ (270.32): C, 75.53; H, 6.71; found C, 75.62; H, 6.69.

(E)-3,5-Dimethoxystilbene (3ab-E). Yield: 764 mg, starting from 610 mg of 3,5-dimethoxybenzaldehyde (87%). Colorless solid, mp 56°C, lit. [35] 55°C. IR (KBr): ν = 3074 (w), 3027 (w), 3001 (w), 2967 (m), 2941 (w), 2842 (w), 1592 (m), 1515 (s), 1464 (m), 1419 (m), 1313 (w), 1268 (s), 1226 (m), 1155 (m), 1140 (m), 1027 (m), 959 (m), 861 (w), 749 (m) cm^{-1}; ^1H NMR (500 MHz, $CDCl_3$): δ = 7.49 – 7.46 (m, 2 H, H-2′+ H-6′), 7.35 – 7.30 (m, 2 H, H-3′ + H-5′), 7.26 – 7.21 (m, 1 H, H-4′), 7.06 (distorted d, *J* = 16.5, 1 H, C*H*=CH), 7.01 (distorted d, *J* = 16.5, 1 H, CH=C*H*), 6.66 (d, *J* = 2.2, 2 H, H-2 + H-6), 6.38 (t, *J* = 2.2, 1 H, H-4), 3.78 (s, 6 H, 2 OCH_3); ^{13}C NMR (126 MHz, $CDCl_3$): δ = 161.0, 139.3, 137.1, 129.2, 128.7, 127.7, 126.6, 104.6, 100.0, 55.3; GC-MS: *m/z* = 240 (100) [M^+], 239 (37), 225 (11), 224 (9), 209 (19), 208 (11), 194 (14), 178 (9), 166 (10), 165 (34), 153 (12), 152 (13); anal. calcd for $C_{16}H_{16}O_2$ (240.30): C, 79.97; H, 6.71; found C, 80.03; H, 7.70.

(E)-3,4′-Dimethoxystilbene (3ba-E). Yield: 847 mg, starting from 500 mg of 3-methoxybenzaldehyde (96%). Colorless solid, mp 109 – 110°C, lit. [35] 108 – 109°C. IR (KBr): ν = 3074 (w), 3027 (w), 3001 (w), 2967 (m), 2941 (w), 2842 (w), 1592 (s), 1515 (s), 1464 (m), 1419 (w), 1312 (w), 1268 (s), 1226 (m), 1155 (w), 1140 (m), 1027 (m), 959 (m), 861 (w), 810 (m), 749 (m) cm^{-1}; ^1H NMR (500 MHz, $CDCl_3$): δ = 7.43 – 7.39 (m, 2 H, H-2′ + H-6′), 7.25 – 7.21 (m, 1 H, H-5), 7.08 – 6.99 (m, 3 H, H-2 + H-6 + C*H*=CH), 6.92 (distorted d, *J* = 16.5, 1 H, CH=C*H*), 6.88 – 6.84 (m, 2 H, H-3′ + H-5′), 6.77 (dd, *J* = 8.2, 2.2, 1 H, H-4), 3.79 (s, 3 H, OCH_3), 3.76 (s, 3 H, OCH_3); ^{13}C NMR (126 MHz, $CDCl_3$): δ = 159.9, 159.3, 139.1, 130.0, 129.6, 128.5, 127.8, 126.5, 119.0, 114.1, 112.9, 111.5, 55.23, 55.16; GC-MS: *m/z* = 240 (100) [M^+], 239 (10), 210 (7), 209 (16), 197 (9), 194 (10), 182 (13), 166 (11), 165 (30), 153 (15), 152 (12); anal. calcd for $C_{16}H_{16}O_2$ (240.30): C, 79.97; H, 6.71; found C, 79.89; H, 6.73.

(E)-4-Methoxystilbene (3cb-E). Yield: 623 mg, starting from 500 mg of 4-methoxybenzaldehyde (81%). Colorless

solid, mp 134–136°C, lit. [35] 134–134.5°C. IR (KBr): ν = 3023 (w), 3004 (w), 2965 (w), 2838 (w), 1603 (m), 1513 (s), 1447 (m), 1297 (w), 1252 (s), 1180 (m), 1031 (s), 968 (m), 860 (w), 813 (m), 750 (s), 689 (m) cm^{-1}; ^1H NMR (500 MHz, $CDCl_3$): δ = 7.48–7.45 (m, 2 H, H-2′ + H-6′), 7.44–7.41 (m, 2 H, H-2 + H-6), 7.34–7.30 (m, 2 H, H-3′ + H-5′), 7.23–7.19 (m, 1 H, H-4′), 7.05 (distorted d, J = 16.5, 1 H, C*H*=CH), 6.95 (distorted d, J = 16.5, 1 H, CH=C*H*), 6.89–6.84 (m, 2 H, H-3 + H-5), 3.78 (s, 3 H, OCH_3); ^{13}C NMR (126 MHz, $CDCl_3$): δ = 159.3, 137.7, 130.1, 128.6, 128.2, 127.7, 127.2, 126.6, 126.3, 114.1, 55.3; GC-MS: m/z = 210 (100) [M^+], 209 (17), 195 (20), 194 (7), 179 (13), 178 (8), 177 (6), 167 (39), 166 (17), 165 (53), 152 (29), 139 (10), 115 (11), 89 (9), 76 (5), 63 (12); anal. calcd for $C_{15}H_{14}O$ (210.27): C, 85.68; H, 6.71; found C, 85.59; H, 6.72.

(E)-3,4′,5-Trihydroxystilbene (4aa-E, trans-RSV). Yield: 293 mg, starting from 386 mg of (*E*)-3,4′,5-trimethoxystilbene (90%). Colorless solid, mp 255–257°C, lit. [35] 256–257°C. IR (KBr): ν = 3289 (s, br), 1603 (m), 1588 (s), 1510 (m), 1456 (w), 1324 (w), 1252 (m), 1154 (m), 965 (m), 830 (m) cm^{-1}; ^1H NMR (500 MHz, DMSO-d_6): δ = 9.57 (s, br, 1 H, OH), 9.23 (s, br, 2 H, 2 OH), 7.43–7.39 (m, 2 H, H-2′ + H-6′), 6.96 (distorted d, J = 16.5, 1 H, C*H*=CH), 6.84 (distorted d, J = 16.5, 1 H, CH=C*H*), 6.80–6.76 (m, 2 H, H-3′ + H-5′), 6.43 (d, J = 2.2, 2 H, H-2 + H-6), 6.16 (t, J = 2.2, 1 H, H-4); ^{13}C NMR (126 MHz, DMSO-d_6): δ = 158.4, 157.1, 139.2, 128.0, 127.81, 127.77, 125.6, 115.5, 104.3, 101.7; MS (direct injection): m/z = 228 (100) [M^+], 227 (18), 213 (4), 211 (10), 210 (5), 199 (5), 182 (4), 181 (14), 165 (4), 157 (4), 152 (4); anal. calcd for $C_{14}H_{12}O_3$ (228.24): C, 73.67; H, 5.30; found C, 73.75; H, 5.28.

(E)-3,5-Dihydroxystilbene (4ab-E). Yield: 242 mg, starting from 343 mg of (*E*)-3,5-dimethoxystilbene (80%). Colorless solid, mp 154–155°C, lit. [35] 157–158°C. IR (KBr): ν = 3289 (s), 1617 (m), 1599 (s), 1588 (s), 1501 (w), 1472 (m), 1358 (w), 1252 (m), 1169 (m), 1148 (m), 1008 (m), 963 (m), 840 (w), 689 (m) cm^{-1}; ^1H NMR (300 MHz, DMSO-d_6): δ = 9.34 (s, 2 H, 2 OH), 7.62–7.56 (m, 2 H, H-2′ + H-6′), 7.41–7.32 (m, 2 H, H-3′ + H-5′), 7.30–7.22 (m, 1 H, H-4′), 7.15–7.03 (AB system, J = 16.9, 2 H, CH=CH), 6.53 (d, J = 2.1, 2 H, H-2 + H-6), 6.26 (t, J = 2.1, 1 H, H-4); ^{13}C NMR (75 MHz, DMSO-d_6): δ = 158.6, 138.8, 137.1, 129.1, 128.6, 127.9, 127.4, 126.4, 104.9, 102.6; MS (direct injection): m/z = 212 (100) [M^+], 211 (36), 197 (10), 195 (7), 194 (6), 193 (5), 183 (4), 181 (2), 165 (12), 153 (2), 141 (2); anal. calcd for $C_{14}H_{12}O_2$ (212.24): C, 79.22; H, 5.70; found C, 79.34; H, 5.68.

(E)-3,4′-Dihydroxystilbene (4ba-E). Yield: 197 mg, starting from 343 mg of (*E*)-3,4′-dimethoxystilbene (65%). Colorless solid, mp 216–218°C, lit. [35] 216–218°C. IR (KBr): ν = 3290 (s), 1616 (m), 1598 (s), 1588 (s), 1501 (w), 1472 (m), 1358 (w), 1252 (m), 1169 (m), 1149 (m), 1008 (m), 963 (m), 840 (w), 689 (m) cm^{-1}; ^1H NMR (300 MHz, DMSO-d_6): δ = 9.58 (s, br, 1 H, OH), 9.39 (s, br, 1 H, OH), 7.45–7.38 (m, 2 H, H-2′ + H-6′), 7.18–6.88 (m, 5 H, H-2 + H-5 + H-6 + CH=CH), 6.80–6.74 (m, 2 H, H-3′ + H-5′), 6.64 (dd, J = 8.1, 2.1, 1 H, H-4); ^{13}C NMR (75 MHz, DMSO-d_6): δ = 157.6, 157.3, 138.9, 129.4, 128.3, 127.7, 125.5, 117.1, 115.6, 114.3, 112.7; MS (direct injection): m/z = 212 (100) [M^+], 211 (25), 197 (10), 195 (7), 195 (13), 194 (8), 193 (11), 183 (10), 181 (11), 177 (8), 167 (6), 166 (7), 165 (33), 153 (8), 63 (5); anal. calcd for $C_{14}H_{12}O_2$ (212.24): C, 79.22; H, 5.70; found C, 79.15; H, 5.72.

(E)-4-Hydroxystilbene (4cb-E). Yield: 168.2 mg, starting from 300 mg of (*E*)-4-methoxystilbene (60%). Colorless solid, mp 196–197°C, lit. [35] 195–196°C. IR (KBr): ν = 3409 (s, br), 1633 (w), 1455 (w), 1372 (m), 1327 (w), 1207 (w), 1075 (m), 929 (m), 903 (m) cm^{-1}; ^1H NMR (300 MHz, DMSO-d_6): δ = 9.61 (s, br, 1 H, OH), 7.57–7.51 (m, 2 H, H-2′ + H-6′), 7.47–7.40 (m, 2 H, H-2 + H-6), 7.38–7.31 (m, 2 H, H-3′ + H-5′), 7.26–7.18 (m, 1 H, H-4′), 7.16 (distorted d, J = 16.4, 1 H, C*H*=CH), 7.02 (distorted d, J = 16.4, 1 H, CH=C*H*), 6.82–6.75 (m, 2 H, H-3 + H-5); ^{13}C NMR (75 MHz, DMSO-d_6): δ = 157.3, 137.6, 128.5, 128.1, 127.8, 126.9, 126.0, 125.2, 115.6; GC-MS: m/z = 196 (100) [M^+], 195 (37), 181 (19), 179 (11), 178 (12), 177 (28), 176 (7), 167 (20), 166 (8), 165 (25), 152 (16), 115 (6), 89 (9), 77 (7), 76 (8), 63 (7); anal. calcd for $C_{14}H_{12}O$ (196.24): C, 85.68; H, 6.16; found C, 85.76; H, 6.15.

(E)-4,4′-Dihydroxystilbene (4dc-E). Yield: 430 mg, starting from 1.04 g of 4-hydroxybenzaldehyde (24%). Off-white solid, mp 297–300°C, lit. [36] 291–292°C. ^1H NMR (300 MHz, DMSO-d_6): δ (ppm) = 9.41 (s, 2 H, 2 OH), 7.33 (BB′ multiplet, 4 H, H-2 + H-6 + H-2′ + H-6′), 6.88 (s, 2 H, HC=CH), 6.72 (AA′ multiplet, 4 H, H-3 + H-5 + H-3′ + H-5′); ^{13}C NMR (75 MHz, DMSO-d_6): δ (ppm) = 157.2, 129.1, 127.8, 125.7, 115.9; GC-MS: m/z = 212 (100) [M^+], 197 (10), 165 (22), 141 (2), 115 (4), 77 (6); anal. calcd for $C_{14}H_{12}O_2$ (212.26): C, 79.22; H, 5.70; found: C, 79.29; H, 5.78.

2.2 Biological assays and molecular modeling

2.2.1 Reagents

E2 was purchased from Sigma–Aldrich and ICI 182,780 (ICI) was obtained from Tocris Chemicals.

2.2.2 Plasmids

Firefly luciferase reporter plasmids used were XETL [37] for ERα and GK1 [38] for the Gal4 fusion proteins. XETL contains the estrogen response element (ERE) from the Xenopus vitellogenin A2 gene (nucleotides –334 to –289), the herpes simplex virus thymidine kinase promoter region (nucleotides –109 to + 52), the firefly luciferase coding sequence, and the SV40 splice and polyadenylation sites from plasmid pSV232A/L-AA5. Gal4 chimeras Gal-ERα, Gal-ER(G521R), Gal-ER(L525A), and Gal-ER(M543A/

L544A) were expressed from plasmids GAL93.ER(G), GAL93.ER(G521R), GAL93.ER(L525A), and GAL93.ER (M543A/L544A), respectively. They were constructed by transferring the coding sequences for the hormone binding domain (HBD) of ERα (amino acids 282 – 595) from HEG0 [37], pCMVhERG521R [39], pCMVhERL525A [39], and a PCR270 mutagenized intermediate with the point mutations M543A-L544A, respectively, into the mammalian expression vector pSCTEVGal93 [40]. The *Renilla reniformis* luciferase expression vector pRL-CMV (Promega) was used as a transfection standard.

2.2.3 Cell culture

Human breast cancer MCF7 cells were maintained in DMEM with phenol red supplemented with 10% FBS. ER-negative SkBr3 human breast cancer cells were maintained in RPMI 1640 without phenol red supplemented with 10% FBS. MCF7 cells to be processed for immunoblot and RT-PCR assays were switched to medium without serum and phenol red 24 h before treatments.

2.2.4 ER binding assay

MCF-7 cells were stripped of any estrogen by keeping them in medium without serum for 2 days. Cells were incubated with 1 nM [2,4,6,7-3H]E2 (89 Ci/mmol; Amersham Bioscience) and increasing concentrations of nonlabeled E2, RSV or each derivative for 1 h at 37°C in a humidified atmosphere of 95% air/5% CO2. After removal of the medium, cells were washed with ice-cold PBS/0.1% methylcellulose twice, harvested by scraping and centrifugation, and lysed with 100% ethanol, 500 µL *per* 60 mm dish, for 10 min at room temperature [41]. The radioactivity of extracts was measured by liquid scintillation counting.

2.2.5 Transfections and luciferase assays

Cells were transferred into 24-well plates with 500 µL of regular growth medium/well the day before transfection. MCF7 cell medium was replaced with DMEM supplemented with 1% charcoal-stripped (CS) FBS lacking phenol red and serum on the day of transfection, which was performed using the Fugene6 Reagent as recommended by the manufacturer (Roche Diagnostics, Mannheim, Germany) with a mixture containing 0.2 µg of reporter plasmid and 1 ng of pRL-CMV. After 5 – 6 h the medium was replaced again with serum-free DMEM lacking phenol red and supplemented with 1% CS-FBS, ligands were added at this point and cells were incubated for 16 – 18 h. SkBr3 cell medium was replaced with RPMI without phenol red and serum on the day of transfection, which was performed using the Fugene6 Reagent with a mixture containing 0.5 µg of reporter plasmid, 1 ng of pRL-CMV, and 0.1 µg of effector plasmid where applicable. After 5 – 6 h ligands were added and cells were incubated for 16 – 18 h. Luciferase activity was then measured with the Dual Luciferase kit (Promega) according to the manufacturer's recommendations. Firefly luciferase activity was normalized to the internal transfection control provided by the *Renilla* luciferase activity.

2.2.6 Reverse transcription and real-time PCR

Total RNA was extracted using Trizol commercial kit (Invitrogen, Milan, Italy) according to the manufacturer's protocol. RNA was quantified spectrophotometrically, and its quality was checked by electrophoresis through agarose gels stained with ethidium bromide. Only samples that were not degraded and showed clear 18S and 28S bands under UV light were used for RT-PCR. Total cDNA was synthesized from the RNA by reverse transcription using the murine leukemia virus reverse transcriptase (Invitrogen) following the protocol provided by the manufacturer. The expression of selected genes was quantified by real-time PCR using Step One (TM) sequence detection system (Applied Biosystems, Milano, Italy), following the manufacturer's instructions. Gene-specific primers were designed using Primer Express version 2.0 software (Applied Biosystems). Assays were performed in triplicate, and the mean values were used to calculate expression levels, using the relative standard curve method. For pS2, Cathepsin D, PR, c-*fos*, Cyclin A, Cyclin D1, and the ribosomal protein 18S, which was used as a control gene to obtain normalized values, the primers were: 5′-GCCCCCCGTGAAAGAC-3k (pS2 forward) and 5′-CGTCGAAACAGCAGCCCTTA-3′ (pS2 reverse); 5′-CTGGATCCACCACAAGTACAACA-3′ (Cathepsin D forward), 5′-CGAGCCATAGTGGATGTCAAAC-3′ (Cathepsin D reverse); 5′-GAGTTGTGAGAGCACTGGATGCT-3′ (PR forward) and 5′-CAACTGTATGTCTTGACCTGGTGAA-3′ (PR reverse); 5′-CGAGCCCTTTGATGACTTCCT-3′ (c-*fos* forward), 5′-GGAGCGGGCTGTCTCAGA-3′ (c-*fos* reverse); 5′-TGCACCCCTTAAGGATCTTCCT-3′ (Cyclin A forward), 5′-GTGAACGCAGGCTGTTTACTGT-3′ (Cyclin A reverse); 5′-GTCTGTGCATTTCTGGTTGCA-3′ (Cyclin D1 forward), 5′-GCTGGAAACATGCCGGTTA-3′ (Cyclin D1 reverse); and 5′-GGCGTCCCCCAACTTCTTA-3′ (18S forward); 5′-GGGCATCACAGACCTGTTATT-3′ (18S reverse).

2.2.7 Immunoblotting

MCF7 cells were grown in 10 cm dishes and exposed to ligands for 18 h before lysis in 500 µL of 50 mM HEPES, pH 7.5, 150 mM NaCl, 1.5 mM MgCl2, 1 mM EGTA, 10% glycerol, 1% Triton X-100, a mixture of protease inhibitors (Aprotinin, PMSF), and Na-orthovanadate. Equal amounts of total protein were resolved on a 10% SDS-polyacrylamide gel. Proteins were transferred to a nitrocellulose membrane, probed with the antibodies F-10 against ERα and β-actin (Santa Cruz Biotechnology), and revealed using the ECL Western Blotting Detection Reagents (GE Healthcare, Amersham).

2.2.8 Proliferation assays

For quantitative proliferation assays 1×10^4 MCF7 cells were seeded in 24-well plates in regular growth medium. Cells were washed once they had attached and further incubated in medium without serum for 24 h. Thereafter, the medium of MCF7 cells was changed and supplemented with 5% CS-FBS. Ligands were added at this point; medium was changed every day (with ligands). On day 6 (after 5 days of treatment), cells were trypsinized and counted using a hemocytometer.

2.2.9 Molecular modeling

(i) preparation of ligands and receptor molecules for docking. Molecular structures of E2, RSV, 4,4′-DHS, 3,5-DHS, 3,4′-DHS, and 4-hydroxystilbene (4-HS) were built and energy minimized with the programs InsightII and Discover3 (Biosym/MSI, San Diego, CA, USA). To model the receptor–ligand complexes, the coordinates of ERα (PDB:1G50) receptor in complex with the corresponding steroid hormone were used. The receptor and the ligands were prepared for docking using ADT, the AutoDock tool graphical interface [42]. For each receptor structure polar hydrogens were added, Kollman charges were assigned and atomic solvatation parameters were added. Polar hydrogen charges of the Gasteiger-type were assigned and the nonpolar hydrogens were merged with the carbons, the internal degrees of freedom and torsions were set for all the designed small molecules. Protein mutations were introduced into the crystallographic structure of ERα using the program O [43]. The resulting atomic models were then submitted to different cycles of molecular dynamics followed by energy minimization using the programs Insight II and Discover3. The resulting models were used as targets for molecular docking simulations using the program AutoDock 3.05. (ii) Docking simulations. In a first phase, each moiety was docked into the active site using the program AutoDock 3.05 [44] with the macromolecule considered as a rigid body and the ligands being flexible. The search was extended over the whole receptor protein. Affinity maps for all the atom types present, as well as an electrostatic map, were computed with a grid spacing of 0.375 Å. The search was carried out with the Lamarckian Genetic Algorithm: populations of 256 individuals with a mutation rate of 0.02 were evolved for 100 generations. Evaluation of the results was performed by sorting the different complexes with respect to the predicted binding energy. A cluster analysis based on root mean square deviation values, with reference to the starting geometry, was subsequently performed and the lowest energy conformation of the more populated cluster was considered as the most promising bioactive candidate. When clusters of molecules were almost equipopulated, and their energy distribution is spread, the corresponding moiety was not considered a good ligand.

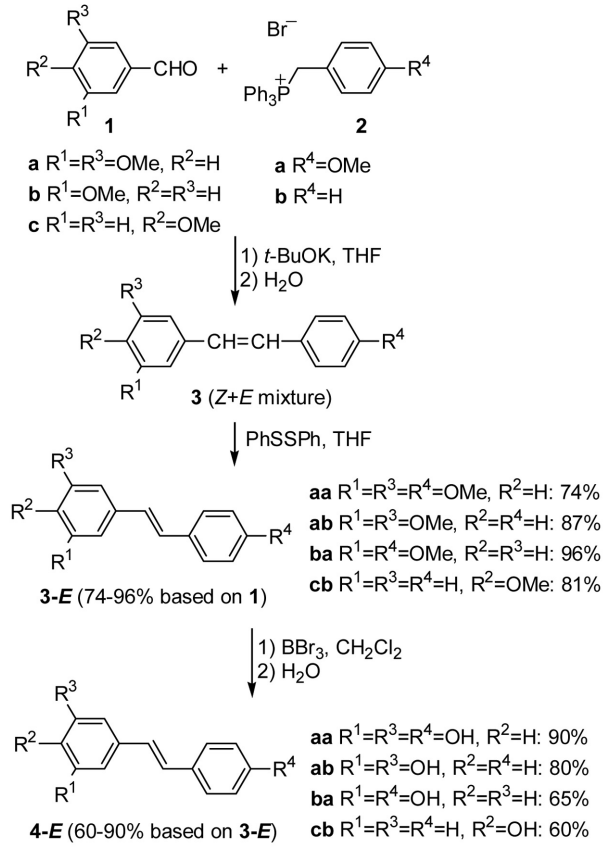

Scheme 1.

All calculations were performed on a Linux workstations equipped with 2 XEON processors, figures were realized with CCP4MG [45].

3 Results and discussion

3.1 Synthesis of Hydroxystilbenes 4aa-*E* (RSV), 4ab-*E* (3,5-DHS), 4ba-*E* (3,4′-DHS), 4cb-*E* (4-HS), 4dc-*E* (4,4′-DHS)

Hydroxystilbenes 4aa-*E*, 4ab-*E*, 4ba-*E*, and 4cb-*E* were prepared by Wittig reaction between the appropriate methoxybenzaldehyde 1a, 1b, or 1c and the appropriate benzyltriphenylphosphonium bromide 2a or 2b followed by isomerization and deprotection, according to Scheme 1. (*E*)-4,4′-dihydroxystilbene 4dc (stilbestrol) was prepared by condensation between 4-hydroxybenzaldehyde 1d′ and 4-hydroxyphenylacetic acid 2c′ followed by decarboxylation, according to Scheme 2. RSV and the analogs were synthesized to evaluate the role of the number of the hydroxyl groups present in the aromatic ring(s) as well as the influence of their relative position on the biological activity exerted by each compound.

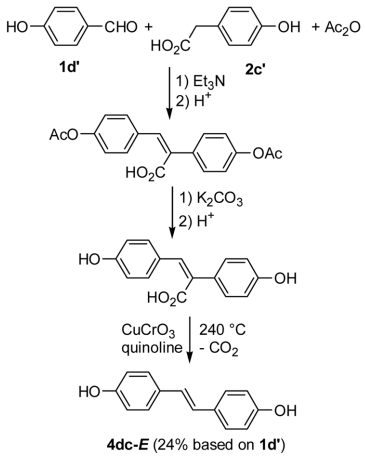

Scheme 2.

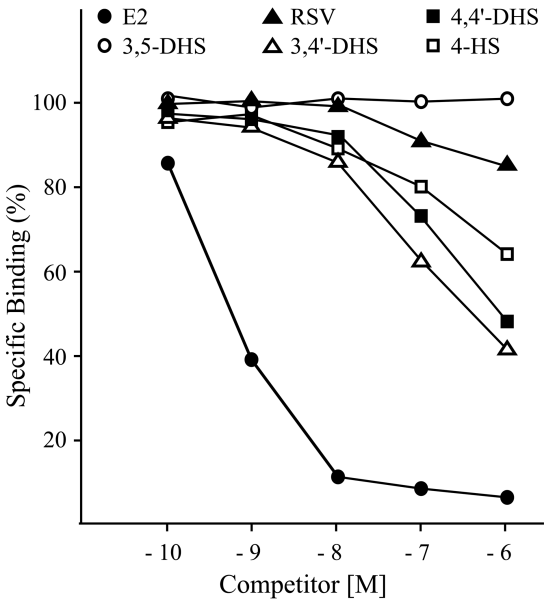

Figure 2. ERα binding assay using increasing concentrations of RSV and analogs. Each point represents the mean of three separate experiments performed in triplicate.

3.2 ERα binding assay

We began our study evaluating whether RSV and derivatives might interact with ERα in extracts of MCF7 cells, which do not express ERβ as judged by RT-PCR (data not shown). Competition binding studies confirmed that RSV is a weak ligand for ERα [20, 21, 46], while all derivatives displayed a higher affinity respect to RSV except 3,5-DHS which did not bind ERα even at the highest concentration used (Fig. 2).

RSV and analogs activate but do not down-regulate endogenous ERα. We then examined whether RSV and the four analogs activate a transiently transfected ER reporter gene (XETL) in MCF7 cells. The reporter plasmid XETL

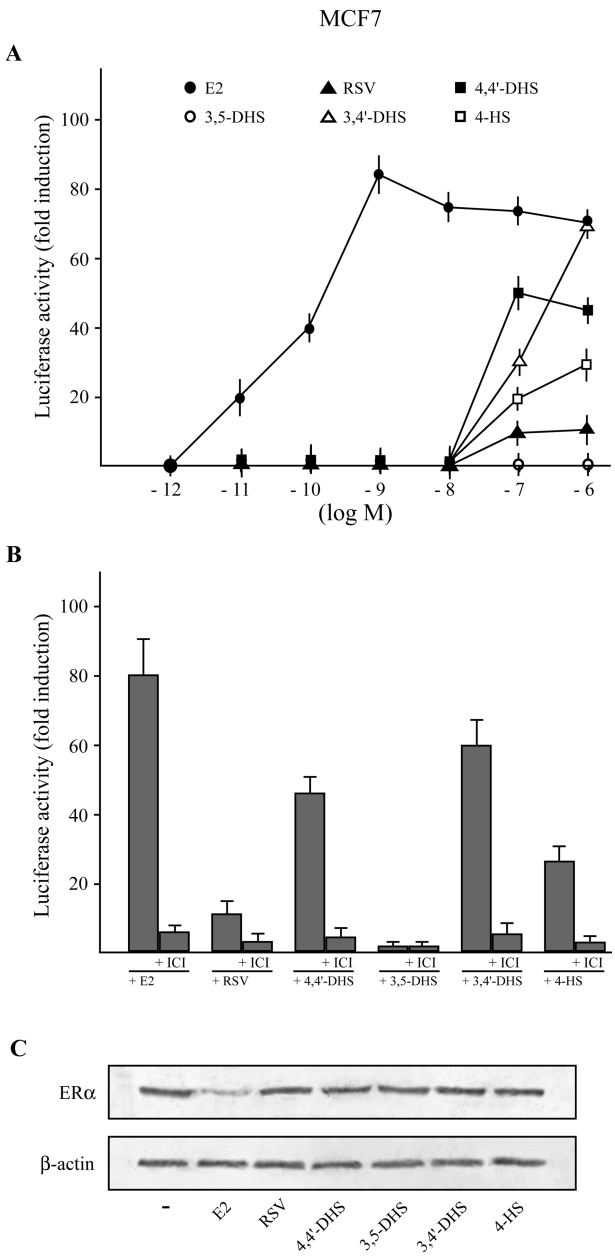

Figure 3. RSV and analogs activate endogenous ERα. (A) MCF7 breast cancer cells were transfected with the luciferase reporter plasmid XETL and treated with increasing concentrations (logarithmic scale) of E2, RSV, and analogs. Luciferase activities were standardized to the internal transfection control and expressed as the ratio of induced activity in absence of ligand. (B) Activation by E2, RSV, and analogs is mediated by ERα. MCF7 cells transfected with the reporter plasmid XETL were treated with 1 nM E2 or 1 μM RSV and analogs with and without 10 μM ER-antagonist ICI. Each data point represents the mean of three experiments performed in triplicate. (C) Immunoblot of ERα from MCF7 cells treated for 24 h with 1 nM E2 or 1 μM RSV and analogs. The results shown are representative of three independent experiments. β-actin serves as loading control.

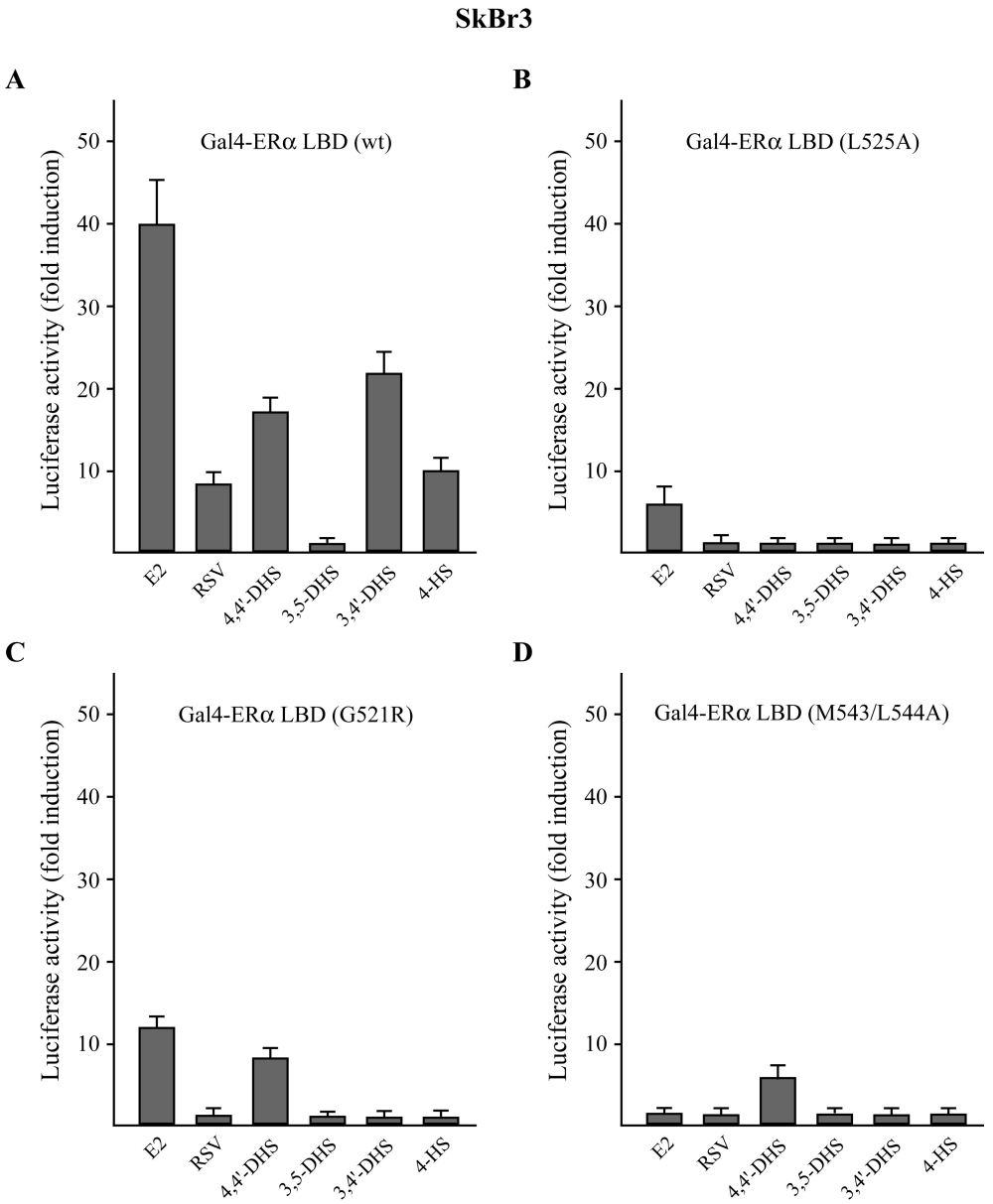

Figure 4. RSV and analogs are ERα agonists in a heterologous system. (A) Fusion proteins consisting of the Gal4 DNA-binding domain and the ERα-LBD are activated by RSV and analogs in transfected SkBr3 breast cancer cells. (B – D) Transactivating response of fusion proteins consisting of the Gal4 DNA-binding domain and ERα-LBD point mutations as indicated. Each data point represents the mean of three experiments performed in triplicate.

carries firefly luciferase sequences under the control of an ERE upstream of the thymidine kinase promoter. As an internal transfection control, we cotransfected a plasmid expressing *Renilla* luciferase, which is enzimatically distinguishable from firefly luciferase, from the strong cytomegalovirus enhancer/promoter. The highest luciferase activity was observed in the presence of 1 nM E2 and 100 pM treatment produced a half maximal stimulation (Fig. 3A). RSV and all the analogs, except 3,5-DHS, were also able to induce luciferase expression, although with lower efficacies compared to E2 even at the highest concentration used, according to the results obtained in competition experiments. Moreover, the transcriptional activity induced by the compounds tested was mediated by ERα since it was no longer evident in the presence of the pure ER antagonist ICI (Fig. 3B). In breast cancer cells, an additional hallmark of full ERα activation by agonists including E2 is represented by the down-regulation of receptor levels through an increased turnover of the E2-activated ERα protein and a reduced transcription of its own gene [47]. Accordingly, a 24 h treatment with 1 nM E2 strongly reduced ERα protein expression in MCF7 cells. RSV and analogs did not show

any modulatory ability at a concentration of 1 μM (Fig. 3C), as recently reported using RSV [48]. Altogether, our results show that, although RSV and three analogs are able to transactivate ERα, they do not trigger all mechanisms involved in ERα down-regulation induced by the cognate ligand E2, likely due to their weak binding affinity for ERα.

3.3 Transcriptional activation of ERα by RSV and analogs in a heterologous system

To examine whether RSV and the analogs transactivate ERα directly, we turned to a completely heterologous system. A chimeric protein consisting of the DNA binding domain (DBD) of the yeast transcription factor Gal4 and the ERα LBD was activated by RSV and all the compounds synthesized, except 3,5-DHS (Fig. 4A) in ER-negative SkBr3 cells. These data demonstrate that the LBD of ERα is sufficient for the transcriptional response and that these compounds act as agonists for the AF-2 domain. We also assessed the response of ERα LBD mutants using Gal4 fusion proteins. The two point mutants L525A and G521R, which require a considerably higher E2 concentration for activation [39], failed to respond to RSV and the analogs, with the exception of the G521R mutant which was sensitive to 4,4′-DHS (Fig. 4B–D). The latter compound also activated the M543/L544A mutant which did not respond to any of the other compounds including E2. These findings suggest that an intact hormone binding pocket of ERα is required for the transactivation elicited by 4,4′-DHS, 3,4′-DHS, and 4-HS whereas in the presence of LBD mutations each compound assumes a particular orientation which may lead to the activation of ERα (see later).

3.4 Docking simulations of wild-type and mutated ERα

The crystal structure of human ERα LBD in complex with its natural ligand E2 (PDB Code 1G50) [49] was used as target for all our docking simulations. Visual inspection of the three dimensional structure of the protein showed that the hormone binding pocket is a mainly hydrophobic buried pocket in which two hydrophilic residues (Arg 394 and His 524) contribute to stabilize the ligand through hydrogen bonds with their hydroxyl groups. The natural ligand E2, RSV and a set of four RSV analogs (Fig. 5) were docked into the hormone binding pocket of ERα to studying the binding modes at a molecular level. In order to investigate the binding of ligands to ERα and evaluate the binding energies of the resulting complexes, we used the computer program AutoDock 3.05/ADT [42, 44]. For each ligand tested, we performed a "blind docking": the docking of small molecules to their targets was done without *a priori* knowledge of the location of the binding site by the system. A preliminary global docking of the natural ligand E2, obtained from the crystal structure of wild-type ERα (PDB code 1G50)

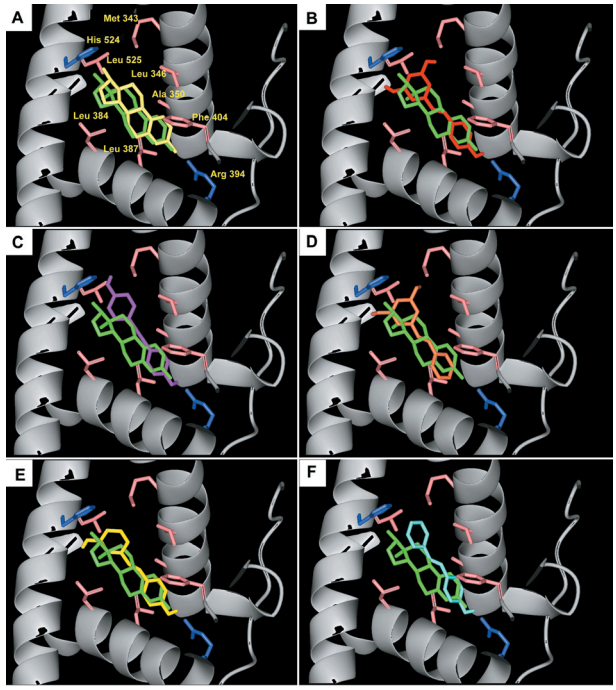

Figure 5. Representation of the binding modes between the tested ligands and ERα, as derived from docking simulations. In all the panels, residues Arg 394 and His 524 involved in hydrogen bond formation with the –OH groups of the ligands, are drawn in blue while hydrophobic residues delimiting the pocket are reported in pink. (A) E2 bound to the ERα, as derived from crystallographic structure (lemon, PDB code:1G50) superposed to the best result of docking simulations (green). (B) RSV (red) superposed to E2 (green). (C) 4,4′-DHS (purple) superposed to E2 (green). (D) 3,5-DHS (tan) superposed to E2 (green). (E) 3,4′-DHS (yellow) superposed to E2 (green). (F) 4-HS (cyan) superposed to E2 (green).

[49], was performed with AutoDock using a grid encompassing the whole protein surface. The docking experiment consisted of 100 simulations which were ranked in order of increasing docking energy values and grouped in clusters with similar conformations (RMSD 0.5 Å). The resulting lowest energy solution was superposed over the crystallographic structure, displaying an RMDS value of 0.112 Å, thus confirming the computational procedure applied with X-ray experiment results. For each compound tested, the solution of docking simulations was grouped by AutoDock in several clusters with comparable binding energies. From the structural analysis of the best solutions (lowest energy) of each cluster, we could highlight differences in the binding orientation. Although the results from AutoDock simulations did not support the hypothesis of a single binding mode, we were able to assess the quality of docked ligands by using, as choice criteria, the evaluation of the hydrophobic contributions as well as visual inspection and comparison of complexes to the crystallographic complex ERα:E2. The final results of docking simulations using the wild-type

Table 1. Hydrogen-bonds and hydrophobic interactions between ligands and the ERα wild-type docking site

	Hydrogen bonds length (Å)			Hydrophobic contacts
	Arg 394	His 524	Leu 525 N-pept.	
E2	2.73	2.71	=	Leu387, Met388, Phe404, Met421, Ile424, Leu525
RSV	2.64	=	=	Leu384, Leu387, Leu391, Phe404, Leu525
4,4′-DHS	2.69	2.78	=	Met343, Leu346, Thr347, Ala350, Leu387, Phe404, Leu525
3,5-DHS	=	=	=	Met343, Leu387, Met388, Leu391, Phe404, Leu525
3,4′-DHS	2.74	3.08	2.97	Met343, Leu387, Phe404, Leu525
4-HS	2.74	=	=	Met343, Thr347, Ala350, Leu387, Phe404, Leu525

Table 2. Affinity constants Ki as calculated by the program AutoDock 3.05

	Wt ERα	G521R	L525A	M543A/L544A
E2	7.7×10^{-9} M	NB	5.2×10^{-8}	8.2×10^{-9}
RSV	3.4×10^{-6} M	NB	NB	3.6×10^{-6}
4,4′-DHS	2.1×10^{-6} M	6.7×10^{-6}	1.7×10^{-5}	2.7×10^{-6}
3,5-DHS	NB	NB	NB	NB
3,4′-DHS	2.1×10^{-6} M	NB	NB	2.8×10^{-6}
4-HS	3.7×10^{-6} M	NB	NB	3.5×10^{-6}

Ki = exp ($\Delta G \times 1000$)/(Rcal × TK) ΔG representing docking energy, Rcal = 1.98719 and TK = 298.15 K, NB = not a ligand.

protein as target, were in good agreement with experimental data, confirming a strong affinity of the protein for E2, a good binding capacity for 4,4′-DHS and 3,4′-DHS ligands, low affinity for RSV and 4-HS, and no affinity for 3,5-DHS (Table 1).

In order to study the mode of binding of RSV analogs, the best docked complexes were subjected to LIGPLOT [50] analysis which allowed us to identify and specify the ligand-protein contacts. Residues involved in ligand binding are reported in Table 1. As expected, the type of interaction is mainly hydrophobic, due to the characteristics of the tested molecules. Two hydrophilic residues (Arg 394 and His 524) are involved in a H-bond through the hydroxyl groups of the bound moieties. The wild-type ERα:E2 complex, as derived from docking simulations, is represented in Fig. 5A; docked E2 (green), resulting from the simulations, is superposed to the crystallographic moiety (purple) for comparison. Panels B-F report the most probable binding mode of the tested ligands (different colors) superposed to the docked E2 (green). Remarkably, some of the residues involved in ligand binding are common for all the tested molecules. The absence of a OH group in one of the two aromatic rings of some moieties, makes the interaction with the target less favored. Being highly hydrophobic and smaller than hormones, these ligands can be accommodated with multiple conformations in the wide binding cavity, mainly lined by hydrophobic residues. Because of these characteristics, the specificity of binding is lower than that for the natural ligand E2.

After performing the simulation using the wild-type protein as target, we attempted to dock the same six ligands on three protein mutants: G521R, L525A, and M543A/L544A, whose structures were built by performing mutations on the coordinates of the wild-type moiety. Table 2 summarizes the results obtained with these new calculations. In particular, the G521R mutation involves the substitution of a residue with a very small side chain (hydrogen atom) with a branched, long and positively charged residue. The cavity hosting the ligand binding site in the wild-type protein is partially occupied by the arginine side chain and therefore the docking simulation indicated only a small affinity for 4,4′-DHS. Docking of E2 on this mutant was not successful, even though we observed a small increase in transcriptional activity. This may be explained considering that in our simulations the protein target is considered as a rigid body whereas real proteins are flexible molecules. The substituted residue R521 could be somehow displaced by the incoming ligand, accommodating some room for binding. Leu525 is important for binding with all the ligands tested here, as reported in Table 1, facilitating hydrophobic contacts between the protein and the skeleton of the ligands thus acting as a "driving force" for the docking. Also in this case, the simulations are in agreement with the *in vitro* tests, displaying a small residual affinity only for E2 to the protein. Different is the case concerning the double mutant M534A/L544A. Although docking simulation reported the same magnitude of activity for the ligands as for the wild-type protein, almost no fold induction was detected *in vitro*. The two mutations, in fact, occur in helix 12, which is not very close to the binding site, however still distant enough to be considered by the docking software as important. At the same time it is known that helix 12 is essential for ER

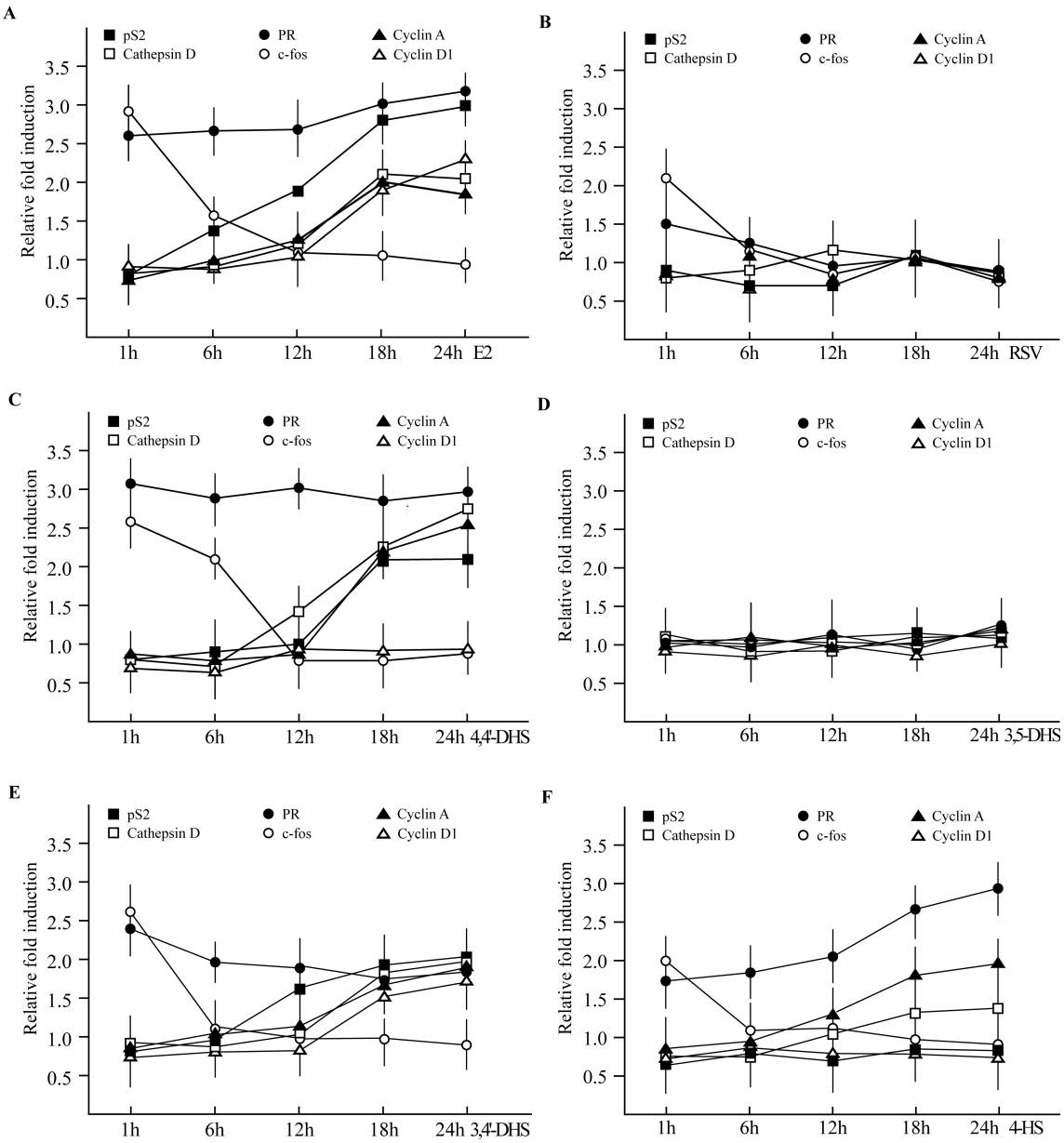

Figure 6. mRNA expression of pS2, Cathepsin D, PR, c-*fos*, Cyclin A and Cyclin D1 evaluated by real-time RT-PCR. MCF-7 cells were treated with vehicle (–), 100 nM E2 (A), 1 μM RSV (B), 4,4′-DHS (C), 3,5-DHS (D), 3,4′-DHS (E), or 4-HS (F) for the indicated times. Results obtained from experiments performed in triplicate were normalized for 18S expression and shown as fold change of RNA expression compared to cells treated with vehicle.

transcriptional activation function. In fact, when an agonist is bound to the ER, helix 12 is oriented anti-parallel to helix 11, capping the ligand binding pocket. This leaves a hydrophobic groove exposed for the binding of coregulator proteins. When an antagonist is bound, helix 12 is displaced via an extended side chain. Helix 12 moves outward, rotates, and packs into the hydrophobic groove between helices 3, 4, and 5. As a result, coactivators needed for transcription cannot bind. What may happen is that this double mutation does not prevent ligand binding, but can perturb the correct displacement of helix 12, thus preventing the binding of cofactors needed for transcription.

3.5 Gene expression changes elicited by RSV and analogs

Having determined that RSV and analogs activate ERα, we evaluated by real-time RT-PCR the potential of each compound to regulate the expression of genes known to be involved in the biological response to estrogens, such as

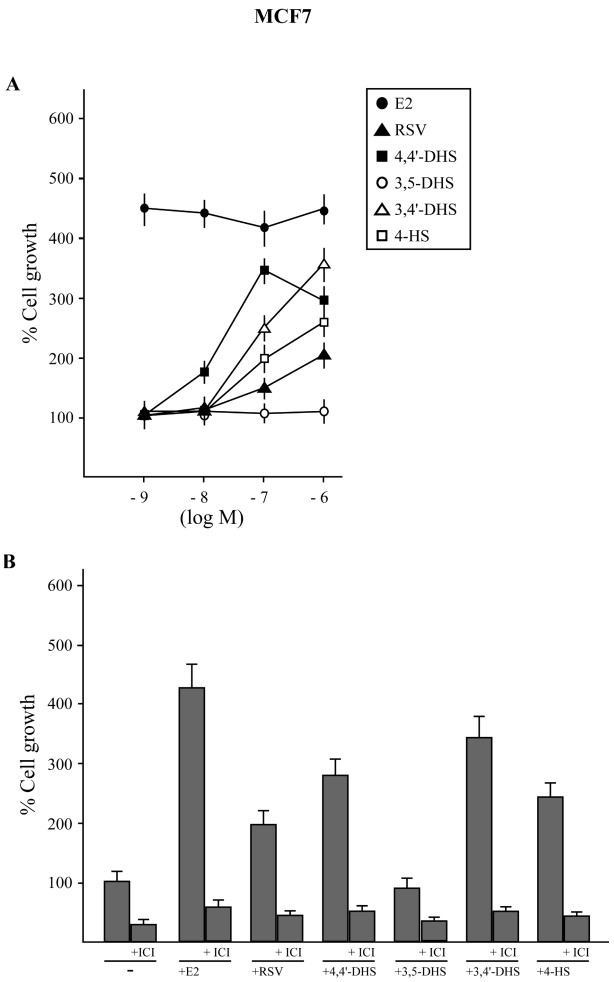

Figure 7. RSV and analogs stimulate proliferative effects in MCF7 breast cancer cells. (A) Cells were treated for 5 days with increasing concentrations (logarithmic scale) of E2, RSV and analogs and counted on day 6. (B) The proliferative effects induced by RSV and analogs are ERα mediated. Cells were treated with 1 nM E2 or 1 μM RSV and analogs with and without 10 μM ER-antagonist ICI. Proliferation of cells receiving vehicle (–) was set as 100% upon which cell growth induced by treatments was calculated. Each data point is the average of three independent experiments.

pS2, Cathepsin D, PR, c-*fos*, Cyclin A, and Cyclin D1 [32–34]. All compounds, except the 3,5-DHS, rapidly (1-h) up-regulated the mRNA expression of PR and c-*fos* (Fig. 6). The expression levels of Cathepsin D, PR, and Cyclin A increased following longer exposures to 4,4′-DHS, 3,4′-DHS, and 4-HS, while pS2 was up-regulated only by 4,4′-DHS and 3,4′-DHS and Cyclin D1 by 3,4′-DHS (Fig. 6). These results suggest that RSV and the analogs studied may have overlapping and yet distinct abilities to regulate the expression of estrogen target genes. Accordingly, it has been reported that different ligands promote distinct molecular conformations and positioning of helix-12 when bound to the ER [32, and references therein]. Interestingly, the latter findings demonstrate that the conformation of the ligand–receptor complex and its ensuing biological activity are tightly connected to the subtle changes in the structure of ligands and not only to dramatic alterations.

3.6 RSV and analogs induce proliferative effects in MCF7 breast cancer cells

On the basis of the above results, we aimed to evaluate a more complex physiological response. We analyzed the effects of RSV and analogs on the proliferation of MCF7 breast cancer cells. Cells were treated for 5 days with increasing concentrations of E2, RSV, and analogs and counted on day 6. Figure 7A shows the results obtained with treatments compared to cells treated with vehicle. RSV and analogs, with the exception of 3,5-DHS, were all able to stimulate the proliferation of MCF7 cells in line with the ability exhibited in transfection experiments. The growth effects elicited by the compounds tested were no longer evident in the presence of the ER antagonist ICI (Fig. 7B), suggesting that ERα mediates cell proliferation in this cell context.

4 Concluding remarks

In the present study, using cell based assays we demonstrated that RSV and analogs exhibit the following order of agonism for ERα: 3,4′-DHS > 4,4′-DHS > 4-HS > RSV. Moreover, the 3,5-DHS derivative did not elicit any ligand activity. Computer modeling indicated that subtle changes in the structure of the compounds examined lead to different binding positions and ERα-LBD conformations which may be responsible for selective gene regulation and growth stimulation in estrogen-sensitive cancer cells.

This work was supported by Associazione Italiana Ricerca sul Cancro (AIRC), Regione Calabria, and Ministero dell'Università.

The authors have declared no conflict of interest.

5 References

[1] Landis, S. H., Murray, T., Bolden, S., Wingo, P. A., Cancer statistics, *CA Cancer J. Clin*. 1999, *49*, 8–31.

[2] Nettles, K. W., Greene, G. L., Ligand control of coregulator recruitment to nuclear receptors, *Annu. Rev. Physiol*. 2005, *67*, 309–333.

[3] Shiau, A. K., Barstad, D., Loria, P. M., Cheng, L., *et al*., The structural basis of estrogen receptor/coactivator recognition and the antagonism of this interaction by tamoxifen, *Cell* 1998, *95*, 927–937.

[4] Heery, D. M., Kakhoven, E., Hoare, S., Parker, M. G., A signature motif in transcriptional co-activators mediates binding to nuclear receptors, *Nature* 1997, *387*, 733–736.

[5] Jensen, E. V., Steroid hormone antagonists. Summary and future challenges, *Ann. N. Y. Acad. Sci*. 1995, *761*, 1 – 4.

[6] Maggiolini, M., Bonofiglio, D., Marsico, S., Panno, M. L., *et al*., Estrogen receptor alpha mediates the proliferative but not the cytotoxic dose-dependent effects of two major phytoestrogens on human breast cancer cells, *Mol. Pharmacol*. 2001, *60*, 595 – 602.

[7] Hill, M. J., Nutrition and human cancer, *Ann. N. Y. Acad. Sci*. 1997, *833*, 68 – 78.

[8] Sinha, R., Potter, J. D., Diet, nutrition, and genetic susceptibility, *Cancer Epidemiol. Biomarkers Prev.* 1997, *6*, 647 – 649.

[9] Messina, M. J., Persky, V., Setchell, K. D., Barnes, S., Soy intake and cancer risk: A review of the *in vitro* and *in vivo* data, *Nutr. Cancer* 1994, *21*, 113 – 131.

[10] Makela, S. I., Pylkkanen, L. H., Santti, R. S., Adlercreutz, H., Dietary soybean may be antiestrogenic in male mice, *J. Nutr.* 1995, *125*, 437 – 445.

[11] Markiewicz, L., Garey, J., Adlercreutz, H., Gurpide, E., *In vitro* bioassays of non-steroidal phytoestrogens, *J. Steroid Biochem. Mol. Biol*. 1993, *45*, 399 – 405.

[12] Sathyamoorthy, N., Wang, T. T., Phang, J. M., Stimulation of pS2 expression by diet-derived compounds, *Cancer Res*. 1994, *54*, 957 – 961.

[13] Stahl, S., Chun, T. Y., Gray, W. G., Phytoestrogens act as estrogen agonists in an estrogen-responsive pituitary cell line, *Toxicol. Appl. Pharmacol*. 1998, *152*, 41 – 48.

[14] Le Bail, J. C., Champavier, Y. M., Chulia, A. J., Habrioux, G., Effects of phytoestrogens on aromatase, 3β and 17β-hydroxysteroid dehydrogenase activities and human breast cancer cells, *Life Sci*. 2000, *66*, 1281 – 1291.

[15] Zava, D. T., Duwe, G., Estrogenic and antiproliferative properties of genistein and other flavonoids in human breast cancer cells *in vitro*, *Nutr. Cancer* 1997, *27*, 31 – 40.

[16] Burns, J., Yokota, T., Ashihara, H., Lean, M. E., Crozier, A., Plant foods and herbal sources of resveratrol, *J. Agric. Food Chem*. 2002, *50*, 3337 – 3340.

[17] Burkon, A., Somoza, V., Quantification of free and protein-bound trans-resveratrol metabolites and identification of trans-resveratrol-C/O-conjugated diglucuronides – Two novel resveratrol metabolites in human plasma, *Mol. Nutr. Food Res*. 2008, *52*, 549 – 57.

[18] Vitaglione, P., Sforza, S., Galaverna, G., Ghidini, C., *et al*., Bioavailability of trans-resveratrol from red wine in humans, *Mol. Nutr. Food Res*. 2005, *49*, 495 – 504.

[19] Bhat, K. P. L., Pezzuto, J. M., Resveratrol exhibits cytostatic and antiestrogenic properties with human endometrial adenocarcinoma (Ishikawa) cells, *Cancer Res*. 2001, *61*, 6137 – 6144.

[20] Bowers, J. L., Tyulmenkov, V. V., Jernigan, S. C., Klinge, C. M., Resveratrol acts as a mixed agonist/antagonist for estrogen receptors α and β, *Endocrinology* 2000, *141*, 3657 – 3667.

[21] Gehm, B. D., McAndrews, J. M., Chien, P. Y., Jameson, J. L., Resveratrol, a polyphenolic compound found in grapes and wine, is an agonist for the estrogen receptor, *Proc. Natl. Acad. Sci. USA* 1997, *94*, 14138 – 14143.

[22] Levenson, A. S., Jordan, V. C., Millennium Review 2000: Selective oestrogen receptor modulation: Molecular pharmacology for the millennium, *Eur. J. Cancer* 1999, *35*, 1628 – 1639.

[23] Mizutani, K., Ikeda, K., Kawai, Y., Yamori, Y., Resveratrol attenuates ovariectomy-induced hypertension and bone loss in stroke-prone spontaneously hypertensive rats, *J. Nutr. Sci. Vitaminol*. 2000, *46*, 78 – 83.

[24] Wu, J. M., Wang, Z. R., Hsieh, T. C., Bruder, J. L., *et al*., Mechanism of cardioprotection by resveratrol, a phenolic antioxidant present in red wine, *Int. J. Mol. Med*. 2001, *8*, 3 – 17.

[25] Hope, C., Planutis, K., Planutiene, M., Moyer, M. P., *et al*., Low concentrations of resveratrol inhibit Wnt signal throughput in colon-derived cells: Implications for colon cancer prevention, *Mol. Nutr. Food Res*. 2008, *52*, 52 – 61.

[26] Mgbonyebi, O. P., Russo, J., Russo, I. H., Antiproliferative effect of synthetic resveratrol on human breast epithelial cells, *Int. J. Oncol*. 1998, *12*, 865 – 869.

[27] Tang, F. Y., Su, Y. C., Chen, N. C., Hsieh, H. S., Chen, K. S., Resveratrol inhibits migration and invasion of human breast-cancer cells, *Mol. Nutr. Food Res*. 2008, *52*, 683 – 691.

[28] Hsieh, T. C., Burfeind, P., Laud, K., Backer, J. M., *et al*., Cell cycle effects and control of gene expression by resveratrol in human breast carcinoma cell lines with different metastatic potentials, *Int. J. Oncol*. 1999, *15*, 245 – 252.

[29] Nakagawa, H., Kiyozuka, Y., Uemura, Y., Senzaki, H., *et al*., Resveratrol inhibits human breast cancer cell growth and may mitigate the effect of linoleic acid, a potent breast cancer cell stimulator, *J. Cancer Res. Clin. Oncol*. 2001, *127*, 258 – 264.

[30] Frémont, L., Biological effects of resveratrol, *Life Sci*. 2000, *66*, 663 – 673.

[31] Le Corre, L., Chalabi, N., Delort, L., Bignon, Y. J., Bernard-Gallon, D. J., Resveratrol and breast cancer chemoprevention: Molecular mechanisms, *Mol. Nutr. Food Res*. 2005, *49*, 462 – 471.

[32] Brooks, S. C., Skafar, D. F., From ligand structure to biological activity: Modified estratrienes and their estrogenic and antiestrogenic effects in MCF-7 cells, *Steroids* 2004, *69*, 401 – 418.

[33] O'lone, R., Frith, M. C., Karlsson, E. K., Hansen, U., Genomic targets of nuclear estrogen receptors, *Mol. Endocrinol.* 2004, *18*, 1859 – 1875.

[34] Sanchez, R., Nguyen, D., Rocha, W., White, J. H., Mader, S., Diversity in the mechanisms of gene regulation by estrogen receptors, *Bioessays* 2002, *24*, 244 – 54.

[35] Ali, M. A., Kondo, K., Tsuda, Y., Synthesis and nematocidal activity of hydroxystilbenes, *Chem. Pharm. Bull*. 1992, *40*, 1130 – 1136.

[36] Schulz, T. P., Hubbard, T. F., Jin, L., Fischer, T. H., Nicholas, D. D., *Phytochemistry* 1990, *29*, 1501 – 1507.

[37] Bunone, G., Briand, P. A., Miksicek, R. J., Picard, D., Activation of the unliganded estrogen receptor by EGF involves the MAP kinase pathway and direct phosphorylation, *EMBO J.* 1996, *15*, 2174 – 2183.

[38] Webb, P., Nguyen, P., Shinsako, J., Anderson, C., *et al*., Estrogen receptor activation function 1 works by binding p160 coactivator proteins, *Mol. Endocrinol*. 1998, *12*, 1605 – 1618.

[39] Ekena, K., Weis, K. E., Katzenellenbogen, J. A., Katzenellenbogen, B. S., Identification of amino acids in the hormone binding domain of the human estrogen receptor important in estrogen binding, *J. Biol. Chem*. 1996, *271*, 20053 – 20059.

[40] Seipel, K., Georgiev, O., Schaffner, W., Different activation domains stimulate transcription from remote ("enhancer") and proximal ("promoter") positions, *EMBO J.* 1992, *11*, 4961 – 4968.

[41] Lee, Y. J., Gorski, J., Estrogen-induced transcription of the progesterone receptor gene does not parallel estrogen receptor occupancy, *Proc. Natl. Acad. Sci. USA* 1996, *93*, 15180 – 15184.

[42] Sanner, M. F., Duncan, B. S., Carillo, C. J., Olson, A. J., Integrating computation and visualization for biomolecular analysis: An example using Python and AVS, *Pac. Symp. Biocomput*. 1999, 401 – 412.

[43] Jones, T. A., Zou, J. Y., Cowan, S. W., Kjeldgaard, M., Improved methods for building protein models in electron density maps and the location of errors in these models, *Acta Crystallogr. A* 1991, *47*, 110 – 119.

[44] Morris, G. M., Goodsell, D. S., Halliday, R. S., Huey, R., *et al*., Automated docking using a lamarkian genetic algorithm and empirical binding free energy function, *J. Computat. Chem*. 1998, *19*, 1639 – 1662.

[45] Potterton, L., McNicholas, S., Krissinel, E., Gruber, J., *et al*., Developments in the CCP4 molecular-graphics project, *Acta Crystallogr. D Biol. Crystallogr*. 2004, *60*, 2288 – 2294.

[46] Ashby, J., Tinwell, H., Pennie, W., Brooks, A. N., *et al*., Partial and weak oestrogenicity of the red wine constituent resveratrol: Consideration of its superagonist activity in MCF-7 cells and its suggested cardiovascular protective effects, *J. Appl. Toxicol*. 1999, *19*, 39 – 45.

[47] Nawaz, Z., Lonard, D. M., Dennis, A. P., Smith, C. L., O'Malley, B. W., Proteasome-dependent degradation of the human estrogen receptor, *Proc. Natl. Acad. Sci. USA* 1999, *96*, 1858 – 1862.

[48] Wu, F., Safe, S., Differential activation of wild-type estrogen receptor alpha and C-terminal deletion mutants by estrogens, antiestrogens and xenoestrogens in breast cancer cells, *J. Steroid Biochem. Mol. Biol*. 2007, *103*, 1 – 9.

[49] Eiler, S., Gangloff, M., Duclaud, S., Moras, D., Ruff, M., Overexpression, purification, and crystal structure of native ER alpha LBD, *Protein Expr. Purif*. 2001, *22*, 165 – 173.

[50] Wallace, A. C., Lawskowski, R. A., Thornton, J. M., LIGPLOT: A program to generate schematic diagrams of protein-ligands interactions, *Prot. Eng*. 1995, *8*, 127 – 134.

